Automated Extraction of Lymph Nodes from 3-D Abdominal CT Images Using 3-D Minimum Directional Difference Filter

Takayuki Kitasaka[1], Yukihiro Tsujimura[1], Yoshihiko Nakamura[1], Kensaku Mori[1], Yasuhito Suenaga[1], Masaaki Ito[2], and Shigeru Nawano[2]

[1] Graduate School of Information Science, Nagoya University, Furo-cho, Chikusa-ku, Nagoya, Aichi, 464-8603, Japan
{kitasaka, kensaku, suenaga}@is.nagoya-u.ac.jp
[2] National Cancer Center Hospital East
Kashiwanoha 6-5-1, Kashiwa, Chiba, 277-8577, Japan

Abstract. This paper presents a method for extracting lymph node regions from 3-D abdominal CT images using 3-D minimum directional difference filter. In the case of surgery of colonic cancer, resection of metastasis lesions is performed with resection of a primary lesion. Lymph nodes are main route of metastasis and are quite important for deciding resection area. Diagnosis of enlarged lymph nodes is quite important process for surgical planning. However, manual detection of enlarged lymph nodes on CT images is quite burden task. Thus, development of lymph node detection process is very helpful for assisting such surgical planning task. Although there are several report that present lymph node detection, these methods detect lymph nodes primary from PET images or detect in 2-D image processing way. There is no method that detects lymph nodes directly from 3-D images. The purpose of this paper is to show an automated method for detecting lymph nodes from 3-D abdominal CT images. This method employs a 3-D minimum directional difference filter for enhancing blob structures with suppressing line structures. After that, false positive regions caused by residua and vein are eliminated using several kinds of information such as size, blood vessels, air in the colon. We applied the proposed method to three cases of 3-D abdominal CT images. The experimental results showed that the proposed method could detect 57.0 % of enlarged lymph nodes with 58 FPs per case.

1 Introduction

Recent progress of medical imaging devices including multi-detector CT scanners has enabled us to take very precise volumetric images of a human in very short time [1,2]. Development of computer-aided diagnosis (CAD) system or computer-assisted surgery (CAS) system, which assists diagnostic process or surgical planning procedure using medical images, is strongly desired. For example, in the case of surgery of colonic cancer, resection of metastasis lesions is

N. Ayache, S. Ourselin, A. Maeder (Eds.): MICCAI 2007, Part II, LNCS 4792, pp. 336–343, 2007.

performed with resection of a primary lesion. Lymph nodes are main route of metastasis and are quite important for deciding resection area. Therefore, diagnosis of enlarged lymph nodes is quite important process for surgical planning. However, manual detection of enlarged lymph nodes on CT images is significantly burden task. Thus, development of lymph node detection process is very helpful for assisting such surgical planning task.

Although there are several reports that present lymph node detection [3,4], these methods detect lymph nodes based on SUV [7] primary from PET images or detect in 2-D image processing way. There is no method that detects lymph nodes directly from 3-D images. Thus, the purpose of this paper is to develop an automated method for detecting lymph nodes from only 3-D abdominal CT images. We employ a 3-D directional difference filter [5] that enhances blob structures and suppresses line structures. The proposed method can detect enlarged lymph nodes only from CT images. This is a big advantage of the proposed method.

2 Method

2.1 Overview

Inputs of the proposed methods are contrasted 3-D abdominal CT images. Normal lymph nodes are quite small. It is quite difficult to find these normal lymph nodes on 3-D CT images. On the other hand, metastasis lymph nodes are enlarged and show spherical shape on 3-D CT images. In the clinical filed, it is important to detect lymph nodes whose diameters are 5mm or higher. So we set the size of a target lymph node as 5mm or higher in diameter.

To enhance blob structure regions, we utilize a 3-D minimum directional difference filter called 3-D Min-DD filter and an extended 3-D Min-DD filter. The 3-D Min DD and the extended 3-D Min-DD filter are kinds of second-order difference filter. Both filters output minimum values of second-order differences with rotating their difference directions. The 3-D Min-DD filter can enhance blob structure regions with suppressing line structure regions. The extended 3-D Min-DD filter can enhance blob structure regions with suppressing curve structure regions. Ability of the extended 3-D Min-DD filter in enhancement of blob structure regions is higher that that of the 3-D Min-DD filter. Since computation time of the extended 3-D Min DD filter is much longer than that of the 3-D Min-DD filter. We apply the extended 3-D Min DD filter only to regions enhanced by the 3-D Min-DD filter. False-positive (FP) reduction process is performed after enhancement by the 3-D Min-DD filter and the extended 3-D Min-DD filter.

The proposed method consist of nine steps: (a) pre-processing, (b) extraction of blob structure, (c) region growing, (d) FP reduction by size, (e) integration of results by detected by filters of different filter sizes, (f) FP reduction using blood vessel information, (g) FP reduction using air region information, (h) removal of small connected components, and (i) FP reductions by degree of sphere.

2.2 Detail Procedures for Lymph Node Detection

(a) Pre-processing
We apply the median filter to an input 3-D abdominal CT image to reduce speckle noise. Then we perform smoothing filtering and obtain the smoothed image $\mathbf{F}$. To eliminate areas of lymph node detection, we extract air regions and bone regions by simple thresholding process. Voxels inside there areas are excluded from the target voxels of lymph node extraction.

(b) Extraction of blob structure region
We apply the 3-D Min-DD filter to all target voxels $\mathbf{p} \in \mathbf{F}$. The 3-D Min-DD filter calculates the directional difference value at $\mathbf{r}(\theta_1, \theta_2)$ and $-\mathbf{r}(\theta_1, \theta_2)$ apart from $\mathbf{p}$ on a sphere with $2r$ in radius as follows.

$$g(\mathbf{p}) = \min_{\theta_1, \theta_2} 2f(\mathbf{p}) - \{f(\mathbf{p} + \mathbf{r}(\theta_1, \theta_2)) + f(\mathbf{p} - \mathbf{r}(\theta_1, \theta_2))\}, \quad (1)$$

where $0 \leq \theta_1 \leq 2\pi$ and $0 \leq \theta_2 \leq 2\pi$. The length of $\mathbf{r}$ controls the size of a target region to be detected. For voxels at which the output of the 3-D Min-DD filter is higher than a given threshold value T_a, we apply the extended 3-D Min-DD filter,

$$h(\mathbf{p}) = \min_{\theta_1, \theta_2, \phi_1, \phi_2} 2f(\mathbf{p}) - \{f(\mathbf{p} + \mathbf{r}(\theta_1, \theta_2)) + f(\mathbf{p} - \mathbf{r}(\theta_1 + \phi_1, \theta_2 + \phi_2))\}, \quad (2)$$

where ϕ_1 and ϕ_2 are parameters for bending the direction of difference, and are set as $-\alpha_1 \leq \phi_1 \leq \alpha_1$ and $-\alpha_2 \leq \phi_2 \leq \alpha_2$, respectively. Then, we binarize the output images with the threshold value T_a and obtain the binary image $\mathbf{B}$.

(c) Region growing
We perform a region growing process starting from voxels $\mathbf{p}$ extracted in (b) to cover whole lymph nodes, since detected regions in (b) are just centers of lymph nodes. The growing condition at a voxel $\mathbf{x}$ is $f(\mathbf{p}) - T_b <= f(\mathbf{x}) <= f(\mathbf{p}) + T_b$, where $f(\mathbf{x})$ denotes a CT value at the voxel $\mathbf{x}$ and T_b is a parameter that controls the range of CT values of voxels which are merged into a region. If this condition is satisfied at the voxel $\mathbf{x}$, $\mathbf{x}$ is merged into the region. The structural element of this region growing is a point (one voxel).

(d) FP reduction by size
The extended 3-D Min-DD filter does not suppress curve structure regions (i.e. blood vessel regions) whose bending angles are sharper than the maximum bending angle of the extended 3-D Min-DD filter (controlled by the parameter α_1 and α_2.) In such regions, resulting regions of the region growing process will become large. So we remove a region whose size is larger than a cube whose edge length is $2r \times 1.5$ [mm] where r is the radius of the 3-D Min-DD or the extended 3-D Min-DD filters.

Table 1. Acquisition parameters of the CT images used in the experiments

Scanner	GE Discovery LS
Num. of pixels	512 × 512
Num. of slices	401 - 451
Pixel size (mm)	0.586
Thickness (mm)	1.25
Recon. pitch (mm)	1.00
Volt (kV)	140
Tube current (mAs)	330

(e) Integration of results
We perform Steps 2.3 to 2.5 by filters of different sizes. Then, extraction results are integrated. Regions detected by these processes are lymph node candidates.

(f) FP reduction using blood vessel information
We remove FP regions by using blood vessel information. First, we enhance line-like structures by utilizing eigenvalues of a Hessian matrix, and extract blood vessel regions by region growing to both original and enhanced intensities [6]. Then, lymph node candidates located inside these blood vessel regions are removed as FP regions.

(g) FP reduction using air region information
FP regions occur around folds or stools of the colon. We use information of these regions for FP reduction. First, we extract regions whose CT values range from -900 H.U. to -200 H.U.. Then, the closing operation of mathematical morphology is applied to the extracted regions. The size of a structural element of the closing operation is 5mm in diameter. Lymph node candidates located inside the extracted regions are removed as FPs.

(h) Removal of small connected components
Small connected components (less than T_c voxels) are also removed as FP regions.

(i) FP reduction by degree of sphere Regions not showing spherical shape are removed in this step. The measure of degree of sphere (DoS) is used to determine its sphericity.

3 Experiments and Discussion

We have applied the proposed method to five cases of 3-D abdominal CT images. Acquisition parameters of CT images are: image size $512 \times 512 \times 401 - 407$, voxel size $0.586 \times 0.586 \times 1.000$ [mm], slice thickness 1.25 [mm], X-ray tube voltage 140 [kV], and tube current 330 [mAs]. We used the 3-D Min-DD filter and the extended 3-D Min-DD filter of 4.0 [mm], 5.0 [mm], and 7.5 [mm] in radius. The

Table 2. TP Rate and Number of FPs

Case No.	Num. of extracted lymph nodes / Num. of lymph nodes specified by radiologists	TP Rate (%)	Num. of FPs
000	22/30	73.3	51
001	44/58	75.9	103
002	15/22	68.2	56
003	20/50	40.0	23
004	25/61	41.0	57
Total	126/221	57.0	290 (58/case)

number of directions of the 3-D Min-DD filter and the extended 3-D Min-DD filter are set as 81 and 6561, respectively. The maximum bending angles α_1 and α_2 of the extended 3-D Min-DD filter are set to 90 [degree]. Threshold value T_a to outputs of the 3-D Min-DD filter and the extended 3-D Min-DD filter is 40 [H.U.]. The parameter T_b used in the region growing process is set to 45 [H.U.]. The parameters T_c and T_d are 50 [voxel] and 8, respectively.

Examples of extracted lymph nodes are shown in Fig. 1. As shown in Fig. 1 (a-d), it is clear that enlarged lymph nodes are extracted successfully. The 3-D views of extracted lymph nodes are shown in Fig. 2. The extraction results are validated by collaborating radiologists. True lymph nodes are specified on CT images. The detection performance is shown in Table 2. The average TP rate was 57.0 % and the average number of FP regions was 58 per case. We conducted ROC analysis of proposed procedures and the results are shown in Fig. 3. After extracting blob structures, there were approx. 17,000 FPs/case while TP rate was 0.89 (indicated the point by arrow in Fig. 3(a)). After region growing, the number of FPs/case was decreased to approx. 600 with 0.66 TP rate (Fig. 3(b)). After removal of small connected components, it was decreased to approx. 250 with 0.63 TP rate (Fig. 3(c)). Finally, after reduction by DoS, it was decreased to 58 with 0.57 TP rate (Fig. 3(d)). The FP reduction process worked effectively using information of size, blood vessel, air, and degree of sphere. The proposed method can detect lymph nodes only from CT images. This is main advantage of the proposed method against other methods. Also, by employing 3-D visualization technique, it is easy to understand the locations of lymph nodes. This 3-D view is quite useful for surgical planning determining resection areas.

Most of FP regions existed on the vein, especially they were found at branching points. This is because we extracted only the artery in the extraction process of blood vessels. FP reduction process using blood vessel information did not work proper for such FPs. Also, CT values of vein regions are quite similar to those of lymph nodes. FPs were detected at branching points of the vein. To reduce such FPs, development of an extraction method of the vein will be one of solutions. Classification based on AdaBoost technique [8] may be another solution.

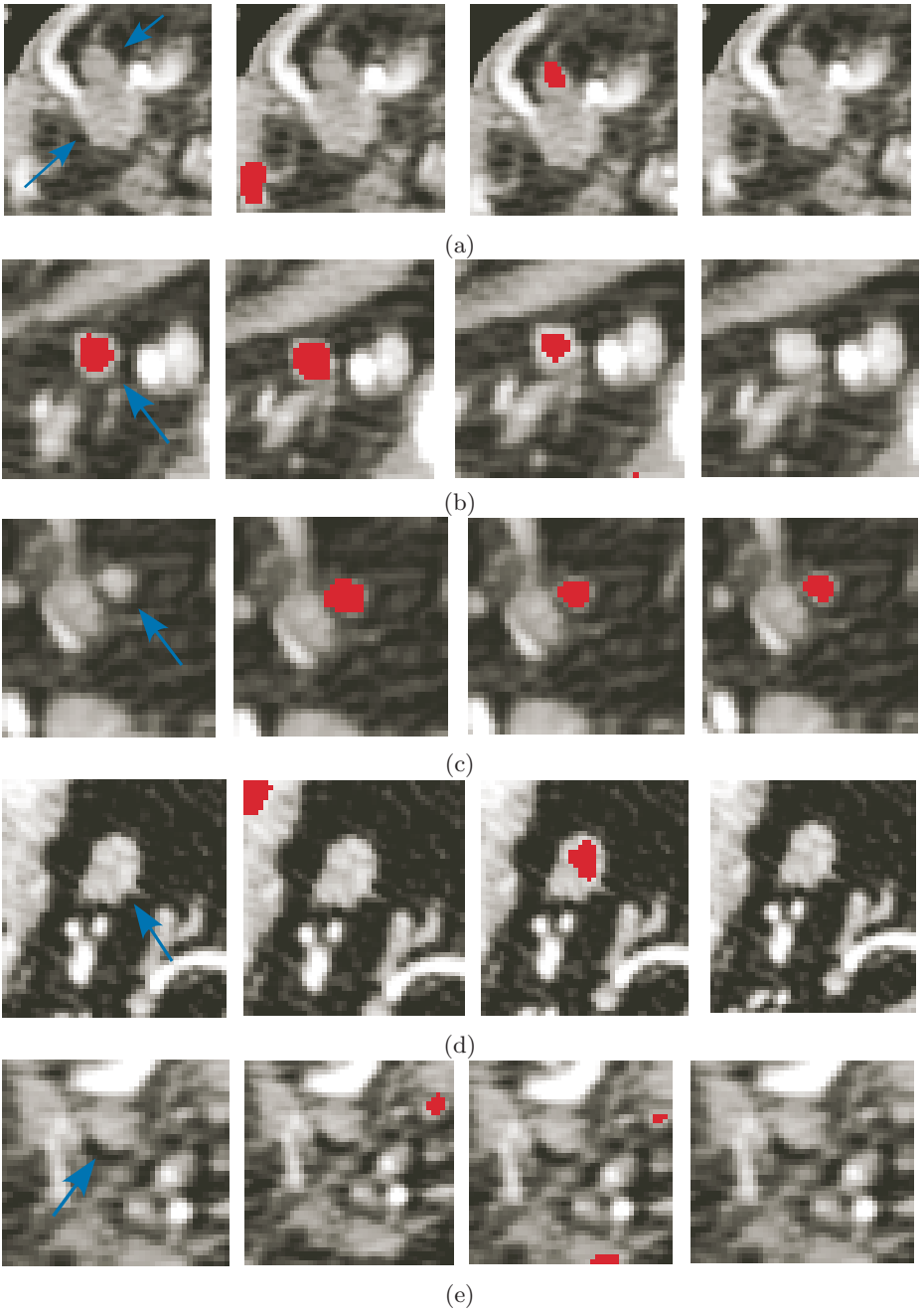

Fig. 1. Results of lymph node detection (arrow: ground truth, red: detected area). Successive slices are shown from left to right for each example. Many enlarged lymph nodes are detected (a-d). However, there are some FNs: larger node in (a) and nodes touching with other tissues in (e) are missing.

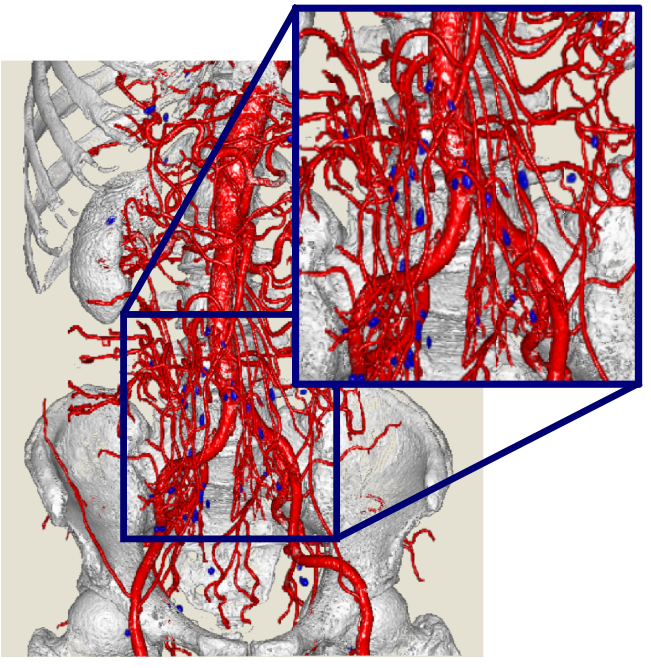

Fig. 2. An example of 3-D display of lymph node detection results

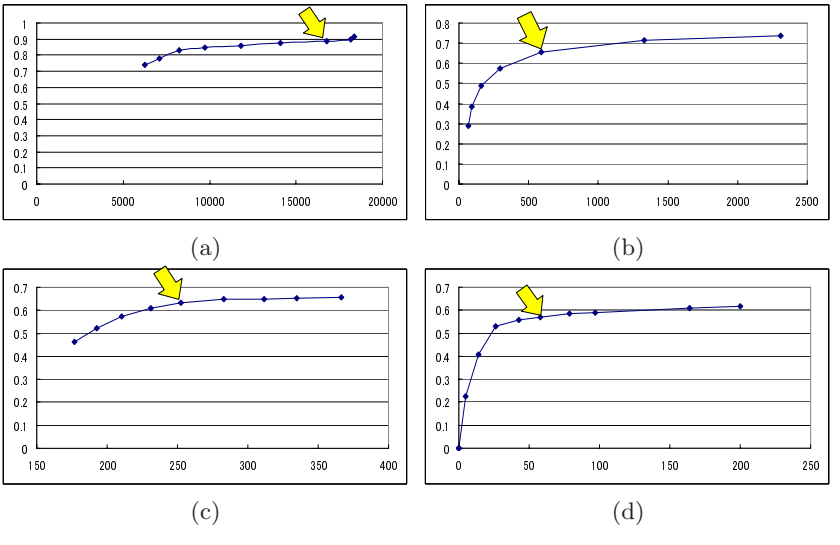

Fig. 3. Results of ROC analysis of each procedure. Horizontal and vertical axes indicate the number of FPs and TP rate, respectively. FROC curves with changing (a) T_a, (b) T_b, (c) T_c, and (d) T_d.

4 Conclusion

This paper presented a method for extracting lymph node regions from 3-D abdominal CT images by using 3-D minimum directional difference filter. The actual procedure consisted of lymph node enhancement using 3-D Min-DD filter and false positive reduction using information of size, blood vessel, air, and degree of sphere. As the results, average TP rate was 57.0% and the average number of FP regions was 58 per case. We believe that the proposed method is quite useful not only for diagnosis of 3-D abdominal CT images but also for surgical planning determining resection areas. Future work includes improvement TP rate with suppressing increase of FPs by modifying the 3-D Min-DD filter and FP reduction procedures, and fusion of detection results from 3-D CT and PET images.

References

1. Shiraishi, S., Tomiguchi, S., Utsunomiya, D., Kawanaka, K., Awai, K., Morishita, S., Okuda, T., Yokotsuka, K., Yamashita, Y.: Quantitative analysis and effect of attenuation correction on lymph node staging of non-small cell lung cancer on SPECT and CT. American Journal of Roentgenology 186, 1450–1457 (2006)
2. Pijl, M.E.J., Chaoui, A.S., Wahl, R.L., van Oostayen, J.A.: Radiology of colorectal cancer. European journal of Cancer 38, 887–898 (2002)
3. Yokoi, N., Shimizu, A., Sato, R., Kobatake, H., Oriuchi, N., Endo, K.: Improvement of the computer-aided detection process of abnormal regions using a combination of PET and CT images. In: Proceedings of JAMIT2006, Op10-2 (2006) (in japanese)
4. Nitta, S., Honda, S., Kasuya, T., Hontani, H., Fukami, T., Yuasa, T., Akatsuka, T., Wu, J., Takeda, T.: Tumor Detection in PET/CT images. IEICE Technical Reports, MI2005, -66 (2006) (in japanese)
5. Shimizu, A., Toriwaki, J.: Characteristics of rotatory second order difference filter for computer aided diagnosis of medical images. Systems and Computers in Japan 26(11), 38–51 (1995)
6. Nakamura, Y., Tsujimura, Y., Kitasaka, T., Mori, K., Suenaga, Y., Nawano, S.: A study on blood vessel segmentation and lymph node detection from 3D abdominal X-ray CT images. In: Proceedings of the 20th International Congress and Exhibition, pp. 381–382 (2006)
7. Sugawara, Y., Zasadny, K.R., Neuhoff, A.W., Wahl, R.L.: Reevaluation of the Standardized Uptage Value for FDG: Variations with Body Weight and Methods for Correction. Radiology 213, 521–525 (1999)
8. Freund, Y., Schapire, R.E.: A decision-theoretic generalization of on-line learning and an application to boosting. Journal of Computer and System Sciences 55 (1997)